Chem

CellPress

Article

Ligand coordination- and dissociation-induced divergent allylic alkylations using alkynes

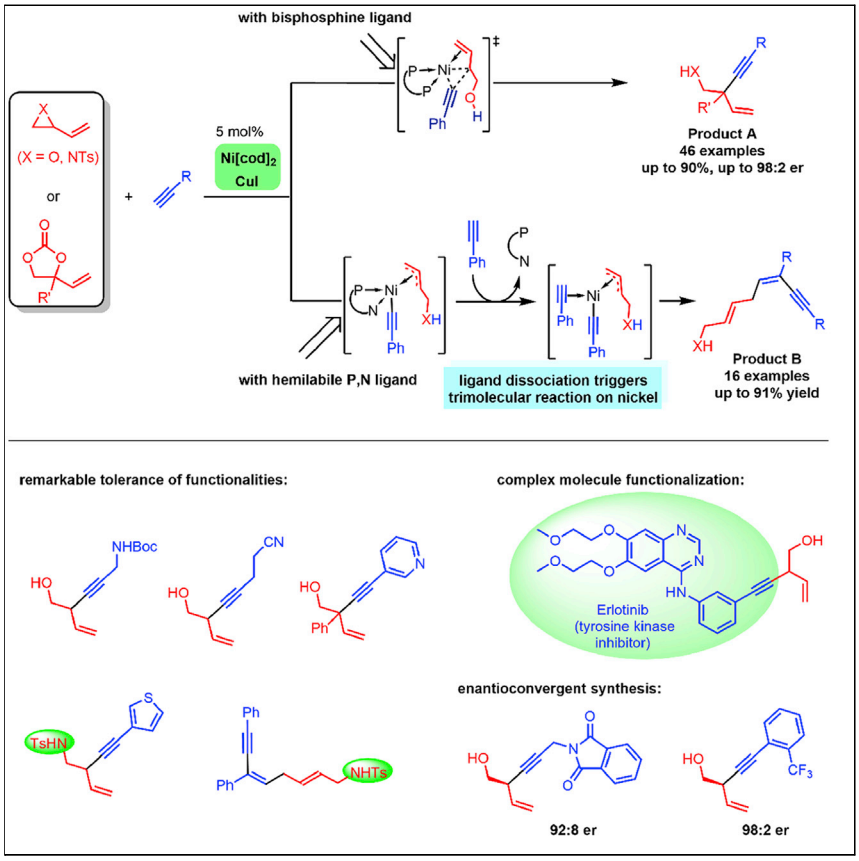

Efficient allylic alkylation of vinyl epoxides/aziridines with terminal alkynes can be achieved in the presence of nickel and copper catalysts. Intriguing ligand-induced divergent reactions are observed to produce either 1,4-enynes from bimolecular allylic alkynylation or dienynes from trimolecular alkyne dimerization/allylic alkylation. The allylic alkynylation reaction works well for a wide range of alkynes bearing a myriad of functionalities. An enantioconvergent transformation of racemic vinyl carbonates to enantioenriched 1,4-enynes is also realized.

Yuan Huang, Chao Ma, Song Liu, Li-Cheng Yang, Yu Lan, Yu Zhao

lanyu@cqu.edu.cn (Y.L.)
zhaoyu@nus.edu.sg (Y.Z.)

HIGHLIGHTS

Ligand coordination/dissociation-induced divergent bimolecular or trimolecular reactions

A general Ni/Cu-catalyzed allylic alkylation of vinyl epoxides/aziridines using alkynes

A remarkable scope of alkynes substituted with a myriad of functionalities

Enantioconvergent allylic alkynylation of vinyl carbonates with alkynes

Huang et al., Chem 7, 812–826
March 11, 2021
https://doi.org/10.1016/j.chempr.2021.02.018

CellPress

Chem

Article

Ligand coordination- and dissociation-induced divergent allylic alkylations using alkynes

Yuan Huang,[1,2,8] Chao Ma,[1,3,8] Song Liu,[4,5,8] Li-Cheng Yang,[1] Yu Lan,[4,6,*] and Yu Zhao[1,7,9,*]

SUMMARY

In transition metal catalysis, the nature of ligand coordination plays a vital role in defining the reactivity of the catalytic system. Achieving multi-substrate coordination and coupling by leveraging dynamic ligand dissociation is rare. Here, we report the discovery of such a phenomenon in nickel/copper-co-catalyzed divergent allylic alkylation of vinyl epoxides and aziridines using alkynes. Under otherwise identical conditions, the use of either strong bisphosphine ligands or hemilabile P,N-ligands leads to bimolecular allylic alkynylation or trimolecular dienyne formation, respectively. DFT calculations provide key insights for these ligand-induced divergent reactivities, particularly ligand-dissociation-enabled coordination of three substrates on nickel for trimolecular coupling. This catalytic system couples a remarkably broad range of readily available terminal alkynes with vinyl epoxides, carbonates, and aziridines in high regio- and stereo-selectivity. The utility of the versatile enyne and dienyne products, coupled with the use of abundant nickel/copper catalysts, makes this a practical method in synthetic and medicinal chemistry.

INTRODUCTION

The efficient generation of compound libraries bearing a broad structural diversity remains an important objective of chemical synthesis in support of medicinal chemistry and material science.[1] As an effective strategy to serve such endeavors, achieving divergent reactivities of the same set of substrates to access different products has attracted much attention in synthetic method development.[2] In particular, transition metal catalysis has given great impetus to delivering elegant examples of chemo-, regio-, or diastereo-divergent transformations to access products that are isomeric in structure.[3–5] In these catalytic methods, it was often the identity of the ligands that played an essential role in altering the steric and electronic properties of the metal complexes leading to different selectivities. It is important to note, however, ligand association on the metal at all times is considered to be the key for efficient catalysis, while the dissociation of ligand typically results in loss of catalytic activity or uncontrolled side reaction pathways. Herein, we present an intriguing yet rarely explored scenario for divergent reactions as shown in Figure 1A: the coordination/dissociation of a ligand may result in different numbers of open binding sites on the metal to accommodate two or more substrates to yield products of completely different molecular scaffolds. By the use of strongly coordinating bidentate ligand, the metal catalyst tends to incorporate only two molecules of substrates and, thus, promotes bimolecular reaction to yield product **A**. Alternatively, the metal complex bearing (hemi)labile ligand may undergo ligand dissociation at an appropriate stage in the catalytic cycle to allow the coordination of more than two substrate molecules, delivering, e.g., product **B** derived from a

The bigger picture

Catalysis is a central concept in chemistry as it enables reactivity not attainable under reasonable conditions by other means and allows for more sustainable and economical processes. In transition metal catalysis, the nature of ligand coordination plays a vital role in the reactivity of the catalytic system. Ligand dissociation from the metal center is typically deemed a destructive scenario, and its alteration to achieve well-controlled reactivity is difficult to accomplish. We report here an intriguing example of leveraging dynamic ligand dissociation on nickel for divergent bimolecular or trimolecular allylic alkylation using terminal alkynes. This catalytic system shows a remarkable scope with superb functional group tolerance and may find wide use in the functionalization of alkyne-containing molecules. This discovery and the detailed mechanistic understanding obtained from DFT calculations will also direct future endeavors in the development of novel, divergent metal-catalyzed reactions.

three-component coupling. To the best of our knowledge, the successful adoption of such a scenario in divergent synthesis remains elusive in the literature. We report herein our discovery and development of Ni and Cu co-catalyzed allylic alkylation of vinyl epoxides and aziridines using terminal alkynes, which represents an interesting example of these ligand coordination- and dissociation-induced divergent transformations, as supported by both experimental observations and detailed DFT calculations.

Transition-metal-catalyzed allylic substitution reactions are of significant utility in organic synthesis.[6–11] Various nucleophiles have been reported to undergo regio- and enantio-selective allylic alkylation, providing access to a wide range of valuable chiral building blocks. However, the use of alkynyl nucleophiles in allylic substitution has remained underdeveloped, even though the 1,4-enyne structure that is accessible from this transformation is a versatile synthon in chemical synthesis. To date, only a few examples of allylic alkynylation were reported under the catalysis of copper or iridium to produce the branched 1,4-enynes in an enantioselective fashion (Figure 1B).[12–16] Alternatively, Pd-catalyzed dehydrative coupling of alkynes with allylic alcohols was also documented to deliver linear 1,4-enynes.[17] However, the products from these systems are limited to simple 1,4-enynes, and the access to related compounds bearing additional functionalities is still highly desired. We were intrigued by this challenge and set out to explore allylic alkynylation of functionalized substrates — such as vinyl epoxides,[18] vinyl ethylene carbonates,[19] and vinyl aziridines[20] — which present attractive, atom-economical access to synthetically versatile alcohol- or amine-containing skipped enynes. Notably, allylic alkynylation of these well-explored substrates with high regio- and stereo-selectivity still remain elusive in the literature. With an aim to promote a more sustainable process, we were particularly interested in the use of terminal alkynes as the nucleophiles and base metals, such as nickel, as the catalysts for our method development.[21]

We report herein not only our development of the first allylic alkynylation of vinyl epoxides, carbonates, and aziridines to yield functionalized branched 1,4-enynes (product **A**; Figure 1C) but also our discovery of ligand-induced switch of reactivity to deliver enyne-containing allyl alcohols and amines (product **B**; Figure 1C). In our studies, dual catalysis of nickel and copper proved to be essential for the high efficiency and selectivity for the reactions, providing an important example of cooperative bimetallic catalysis[22,23] using nonprecious metals. The remarkable scope of this system, the use of commercially available alkynes, and the abundance of nickel and copper catalysts make this a practical method in chemical synthesis. Highly enantioselective allylic alkynylation has also been achieved. Importantly, DFT calculations provided key insight on the cause of this divergent bimolecular or trimolecular reactivities, making it a remarkable demonstration of the effect of ligand coordination and dissociation on substrate participation in transition metal catalysis.

RESULTS AND DISCUSSION

Establishing divergent allylic alkylation of vinyl epoxide using alkynes

To identify an efficient and regioselective catalytic system for allylic alkynylation, we decided to first explore reactions using the strong nucleophile potassium alkynyltrifluoroborate **2a** with vinyl epoxide **1a**. Despite the fact that much work has been done on vinyl epoxides,[24] highly regio- and stereo-selective transition-metal-catalyzed allylic alkylation using carbon-based nucleophiles is still underdeveloped.[25,26] The representative optimization studies are summarized in Figure 2A. Out of the various metal complexes examined, the use of cobalt/scandium salts or $Pd_2(dba)_3$

[1]Department of Chemistry, National University of Singapore, 3 Science Drive 3, Singapore 117543, Singapore

[2]School of Pharmacy, Xi'an Jiaotong University, No. 76, Yanta West Road, Xi'an 710061, China

[3]Ministry of Education Key Laboratory for the Synthesis and Application of Organic Functional Molecules, College of Chemistry and Chemical Engineering, Hubei University, Wuhan 430062, China

[4]School of Chemistry and Chemical Engineering and Chongqing Key Laboratory of Theoretical and Computational Chemistry, Chongqing University, Chongqing 400030, China

[5]Chongqing Key Laboratory of Environmental Materials and Remediation Technologies, Chongqing University of Arts and Sciences, Chongqing 402160, China

[6]College of Chemistry and Institute of Green Catalysis, Zhengzhou University, Zhengzhou 450001, China

[7]Joint School of National University of Singapore and Tianjin University, International Campus of Tianjin University, Binhai New City, Fuzhou 350207, China

[8]These authors contributed equally

[9]Lead contact

*Correspondence: lanyu@cqu.edu.cn (Y.L.), zhaoyu@nus.edu.sg (Y.Z.)

https://doi.org/10.1016/j.chempr.2021.02.018

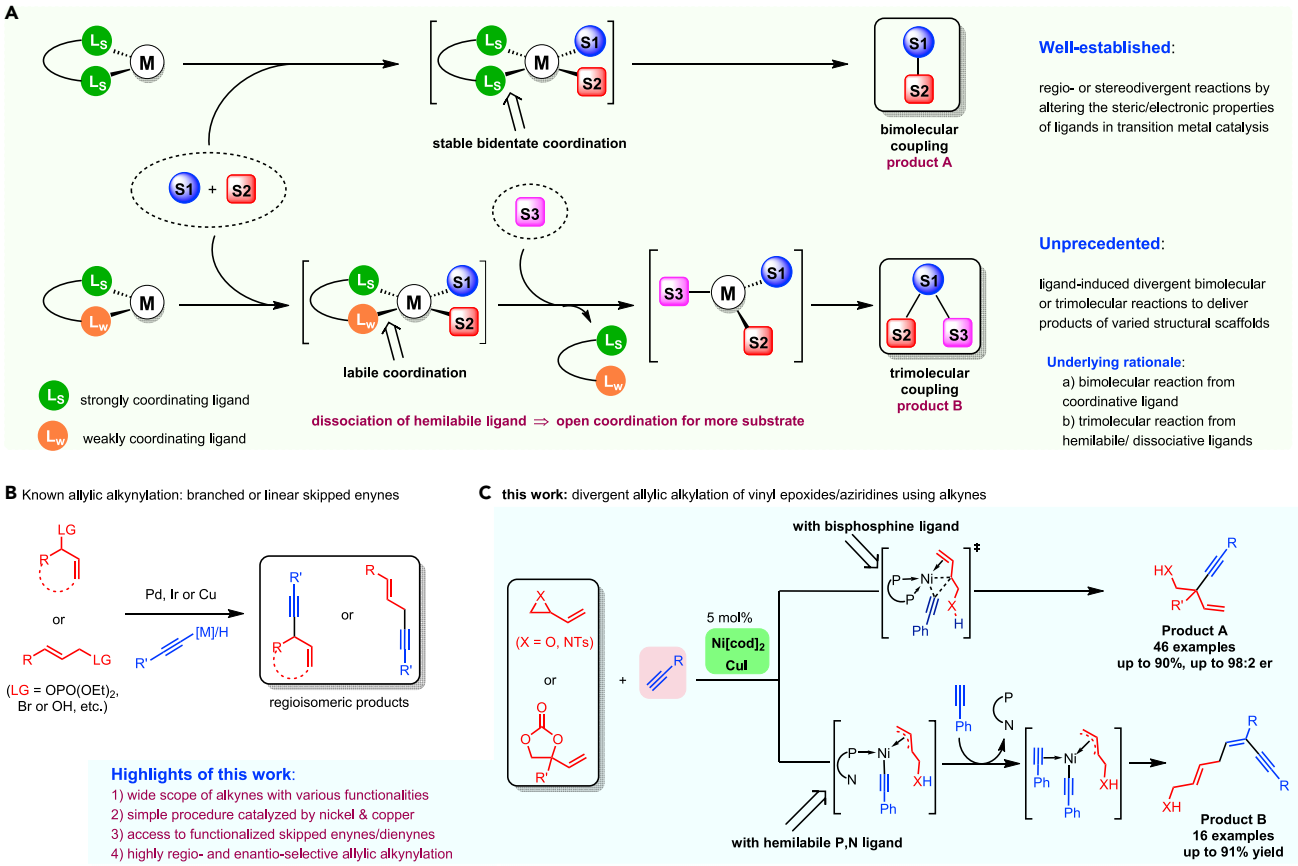

Figure 1. Divergent reactivities induced by coordination or dissociation of ligands

(A) Bimolecular versus trimolecular divergent reactivities determined by the nature of ligand coordination.

(B) Previous allylic alkynylation delivered linear or branched isomeric skipped enynes.

(C) Our discovery of ligand-induced Ni-catalyzed allylic alkylation of vinyl epoxides, carbonates, and aziridines using alkynes: bimolecular allylic alkynylation with strongly coordinating bisphosphine ligand versus trimolecular alkyne dimerization/allylic vinylation with hemilabile P,N-ligand.

led to no reaction at all, whereas using CuI, $Ni[cod]_2$, or $NiBr_2$ resulted in moderate reactivity and poor regioselectivity. When $PdCl_2(PPh_3)_2$ was used, a perfectly branched regioselectivity could be realized; however, the efficiency remained low. To our delight, high reactivity and regioselectivity could be observed in the presence of $NiCl_2(PPh_3)_2$ to yield **3a** in a high yield of 73%.

With the nickel catalysis for allylic alkynylation of **1a** established, we then switched to exploring our desired transformation between **1a** and commercially available alkynes, which possesses much practical advantage (Figure 2B). We first examined the reaction of **1a** with phenylacetylene **5a** by using $NiCl_2(PPh_3)_2$ or $Ni[cod]_2$ together with CuI as a co-catalyst for alkyne activation. Unfortunately, no conversion to the desired product was observed at all. Through a systematic screening of various conditions, we were excited to find out that the ligand had a significant effect on the reactivity. By the use of DPPP with $Ni[cod]_2$ and CuI, the alkynylation proceeded smoothly to deliver **3a** and **4a** in good yields but in a moderate branch to linear ratio (66% versus 17%, first column in Figure 2B). Control reactions were carried out to examine the effect of the dual catalysts at this point (second and third columns in Figure 2B). The reaction without CuI only proceeded to a lower conversion, although the regioselectivity of this reaction remained the same (39% and 10% for **3a**

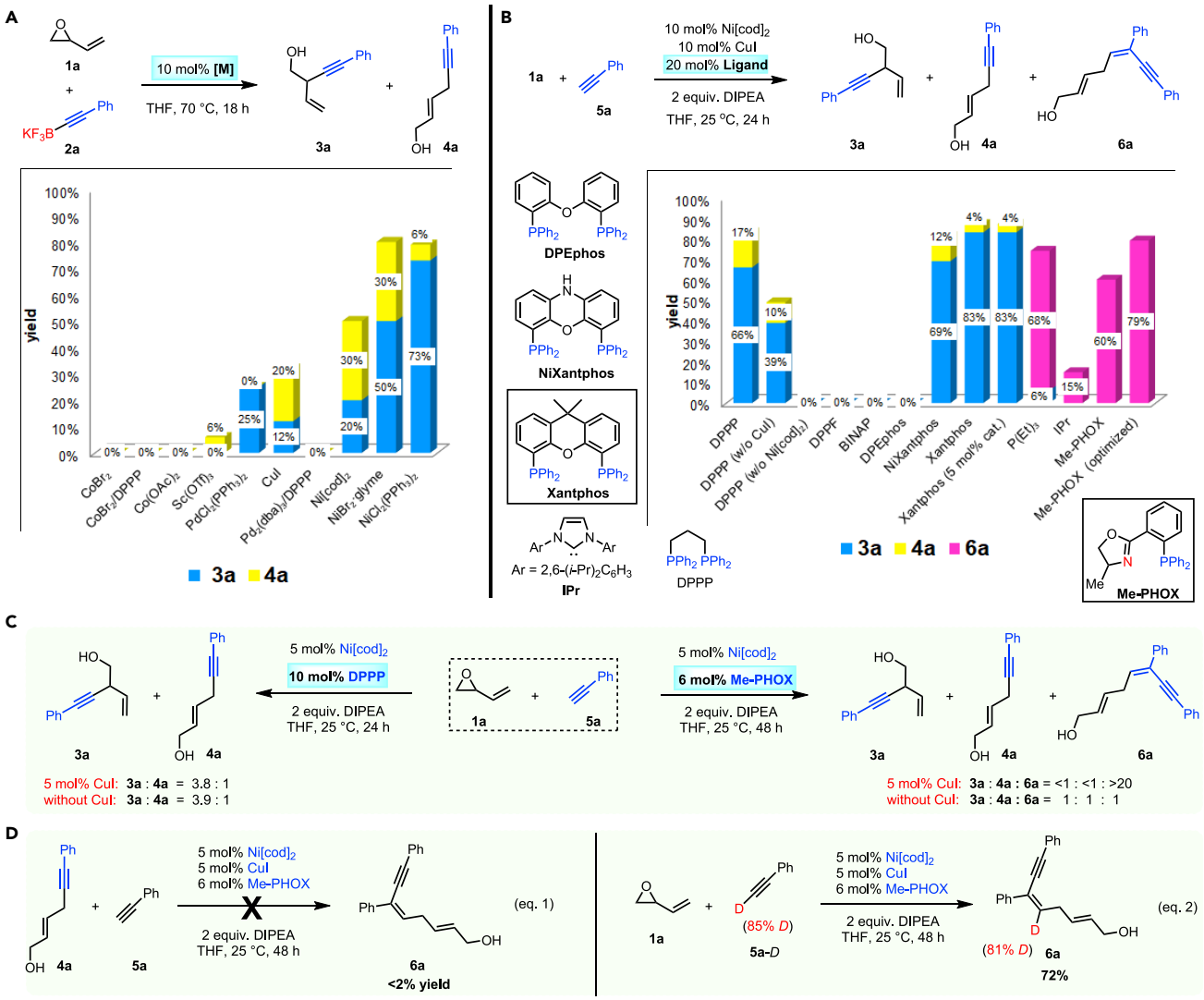

Figure 2. Discovery, optimization, and control experiments for divergent synthesis

(A) Validation of different metals to promote allylic alkynylation of vinyl epoxide using alkynyltrifluoborate **2** identified nickel as an optimal choice.

(B) Examination of various ligands for Ni/Cu bimetallic catalysis identified divergent reactions to deliver **3a** or **6a**. While stable bidentate ligands favored the formation of **3a/4a**, the use of mono-dentate or hemilabile bidentate ligands led to the formation of trimolecular reaction product **6a**.

(C) The presence of copper co-catalyst in the reactions using DPPP ligand led to only improved reactivity with the same level of regioselectivity for allylic alkynylation. In sharp contrast, the presence of copper in the reactions using P,N-ligand completely changed a non-selective formation of three products to, exclusively, formation of **6a**.

(D) Control reactions for the formation of **6a**. The attempted reaction of **4a** and **5a** under the standard conditions led to no formation of **6a**, which ruled out the possibility of a hydroalkynylation of **4** for the formation of **6**. The use of deuterated **5a** led to a clean conversion to **6a** with deuterium on the enyne alkene, which is consistent with alkyne dimerization followed by allylic alkylation mechanism leading to **6a** formation.

and **4a**, respectively). In contrast, no reaction was observed at all in the absence of Ni[cod]$_2$, which should be involved in the key Ni-π-allyl intermediate formation. Clearly, the Ni/Cu dual catalysis was needed to achieve high efficiency in this allylic alkynylation.

In order to further improve the regioselectivity to favor the branched product **3a**, a more thorough screening of ligands was carried out. While the commonly used bisphosphines such as DPPF, BINAP, and DPEPhos completely shut down the alkynylation reaction, the use of NiXantphos with a relatively large bite angle resulted in much higher

regioselectivity (69% and 12% for **3a** and **4a**). The use of Xantphos further enhanced the regioselectivity (~20:1 ratio) and produced **3a** in a high yield of 83%. The catalyst loading was successfully reduced to 5 mol % Ni/Cu and 10 mol % Xantphos to yield **3a** with the same yield and regioselectivity (last blue column in Figure 2B).

Based on these results, we were curious whether the use of more flexible ligands could lead to selective formation of the linear product **4a**. Surprisingly, an intriguing switch of reactivity to produce an enyne-containing allyl alcohol **6a** was observed by the use of monodentate $P(Et)_3$ or N-heterocyclic carbene ligand IPr (first two pink columns in Figure 2B). Further screening of other types of ligands identified the P,N-ligand Me-PHOX as the optimal choice, which produced **6a** exclusively. Under optimized conditions using a lower catalyst loading of 5 mol % with extended reaction time of 48 h and 3:1 ratio of **5a** versus **1a**, desired product **6a** was obtained in a good yield of 79% (last pink column in Figure 2B).

Control experiments were carried out to shed light on the operating mechanism of this Ni-catalyzed divergent allylic alkylation using terminal alkynes. As shown in Figure 2C, by the use of bisphosphine ligands such as DPPP, the CuI co-catalyst only improved the efficiency while maintaining the regioselectivity. In sharp contrast, while a Ni/Cu cooperative system using Me-PHOX as the ligand produced **6a** exclusively, the omission of CuI led to a complete loss of selectivity, resulting in a ~1:1:1 ratio of **3a**, **4a**, and **6a**. The effect of copper is clearly crucial for this transformation.

More control experiments provided some evidence for the mechanism of **6a** formation (Figure 2D). Hypothetically, **6a** should be formed through an alkyne dimerization followed by terminal allylic alkylation. To rule out an alternative sequence of terminal allylic alkynylation followed by hydroalkynylation of the internal alkyne intermediate, we attempted the reaction of pre-synthesized terminal allylic alkynylation product **4a** with **5a** under the standard Ni/Cu-catalyzed conditions. As shown in Equation 1, no formation of **6a** was observed at all, which disfavored the possibility of a late hydroalkynylation step. In addition, deuterium labeled **5a** was subjected to the standard reaction, leading to the formation of **6a** with a clean deuterium labeling at the vinylic position. This was also consistent with the mechanism of alkynylnickelation of a terminal alkyne before allylic alkylation.

Understanding divergent allylic alkylations using DFT calculations

To further probe the underlying causes of these divergent reactivities, we carried out DFT[27] calculations to investigate the mechanism for the formation of **3a**, **4a,** and **6a** for this Ni-catalyzed allylic alkylation reaction. The calculated results are shown in Figures 3 and 4.

The mechanism for the formation of **3a** and **4a** catalyzed by Xantphos-Ni was calculated first. The calculated Gibbs energy profiles for **3a** versus **4a** formation are given in Figure 3, where Xantphos-Ni(0) species **A** was set as the relative zero point. Ligand exchange of vinyl epoxide **1a** with cyclooctadiene in **A** gave π-complex **B** with 8.8 kcal/mol exergonic. The subsequent oxidative addition of vinyl epoxide onto Ni(0) center occurred via transition state with an energy barrier of 13.0 kcal/mol, from which the penta-coordinate allyl-Ni(II) intermediate **C** was generated. At this stage, the Ni-complex could engage alkyne **5a** directly to form the nickel acetylide intermediate **D** through **TS2** with a free energy barrier of 18.1 kcal/mol. In this step, the alkoxide moiety served an important role as base for the deprotonation of **5a**. Alternatively, the inclusion of copper co-catalyst as a π-acid to **5a** (in the form of **E**) greatly facilitated the deprotonation by Ni-alkoxide **C** via **TS3** with a minimal

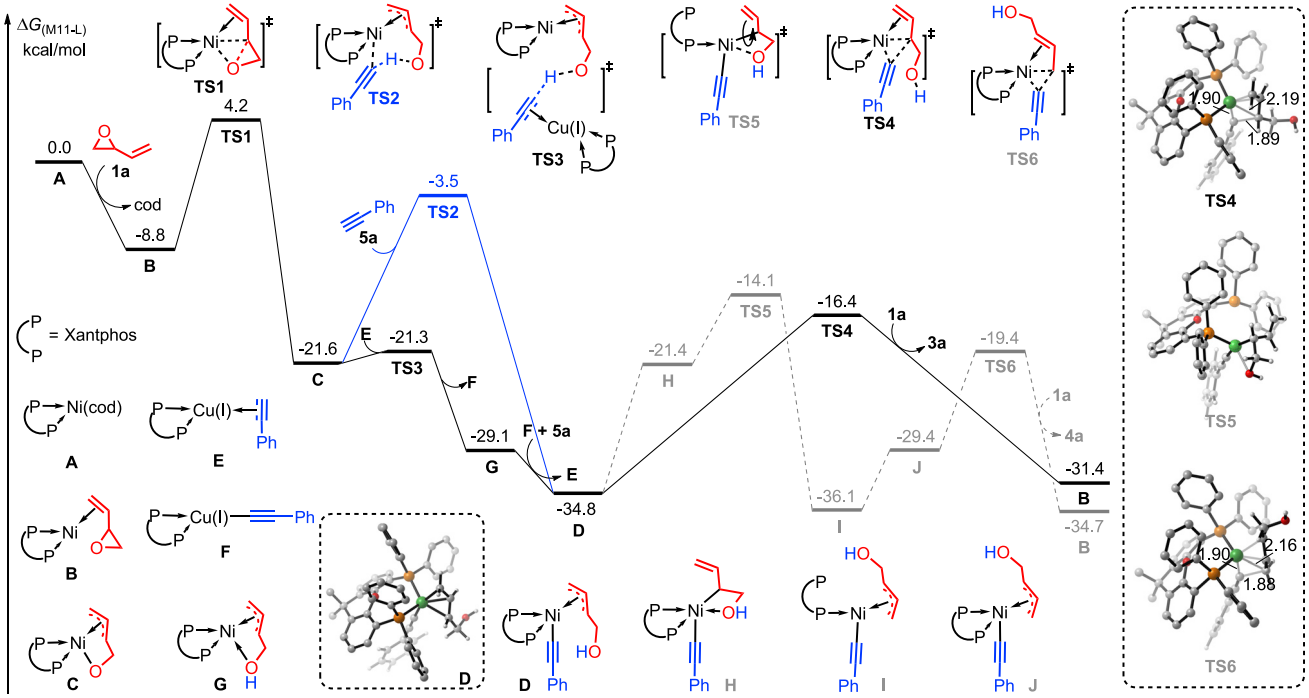

Figure 3. DFT calculations on 3a versus 4a formation catalyzed by Ni/Cu-Xanthpos

Following the formation of Ni-π-allyl alkoxide complex **C**, incorporation of Cu-alkyne complex **E** proceeds via alkoxide base-assisted ligand exchange to give Ni-acetylide **D**. At this stage, direct C(alkynyl)-C(allyl internal) reductive elimination takes place via **TS4** to produce **3a**. For the formation of alternative regioisomer **4a**, a conformational change is required via **H** and **TS5** to generate Ni-π-allyl acetylide complex **I/J** before reductive elimination can take place. This provided a convincing rationale for the regio-selectivity (**3** versus **4**) for Ni-catalyzed allylic alkynylation.

activation barrier of 0.3 kcal/mol; the resultant intermediate **G** then underwent transmetalation with alkynyl copper **F** to yield alkynyl nickel **D** exergonic. The(alkynyl)-C(allyl internal) reductive elimination then took place via **TS4** with a barrier of 18.4 kcal/mol to give the internal alkylation product **3a**. In **TS4**, the length of forming C(alkynyl)-C(allyl internal) bond is 1.89 Å. Ligand exchange of vinyl epoxide **1a** with product **3a** then gave intermediate **B** to complete the catalytic cycle.

For the formation of linear product **4a**, direct reductive elimination of intermediate **D** using the terminal carbon on the allyl unit was not viable due to the anti-relationship of C(alkynyl) and C(allyl terminal). A conformational change had to take place first. As shown by the gray potential energy surface in Figure 3, a ligand exchange between hydroxyl and terminal alkenyl in intermediate **D** gave complex **H** with 13.4 kcal/mol endergonic. The subsequent rotation of allyl unit in **H** then occurred via **TS5**, with an free energy barrier of 7.3 kcal/mol, to generate the allyl-Ni(II) complex **I**, which readily converted to **J**. The relatively high activation barrier in this step (**D** to **I**) is most likely due to the involvement of a Ni-complex in which only one phosphine in Xantphos kept coordination. The following C(alkynyl)-C(allyl) reductive elimination then occurred via **TS6** with a barrier of 10.0 kcal/mol to give the terminal alkylation product **4a**. In **TS6**, the length of forming C(alkynyl)-C(allyl) bond is 1.88 Å. These calculated results show that the relative energy of **TS5** is 2.3 kcal/mol higher than that of **TS4**, which is fully consistent with the experimental observations that **3a** was formed as the major regioisomer (**3a**:**4a** ~20:1).

DFT calculations were also carried out to better understand the mechanism for **6a** formation by the use of Ni-MePHOX in combination with CuI (Figure 4). On the basis

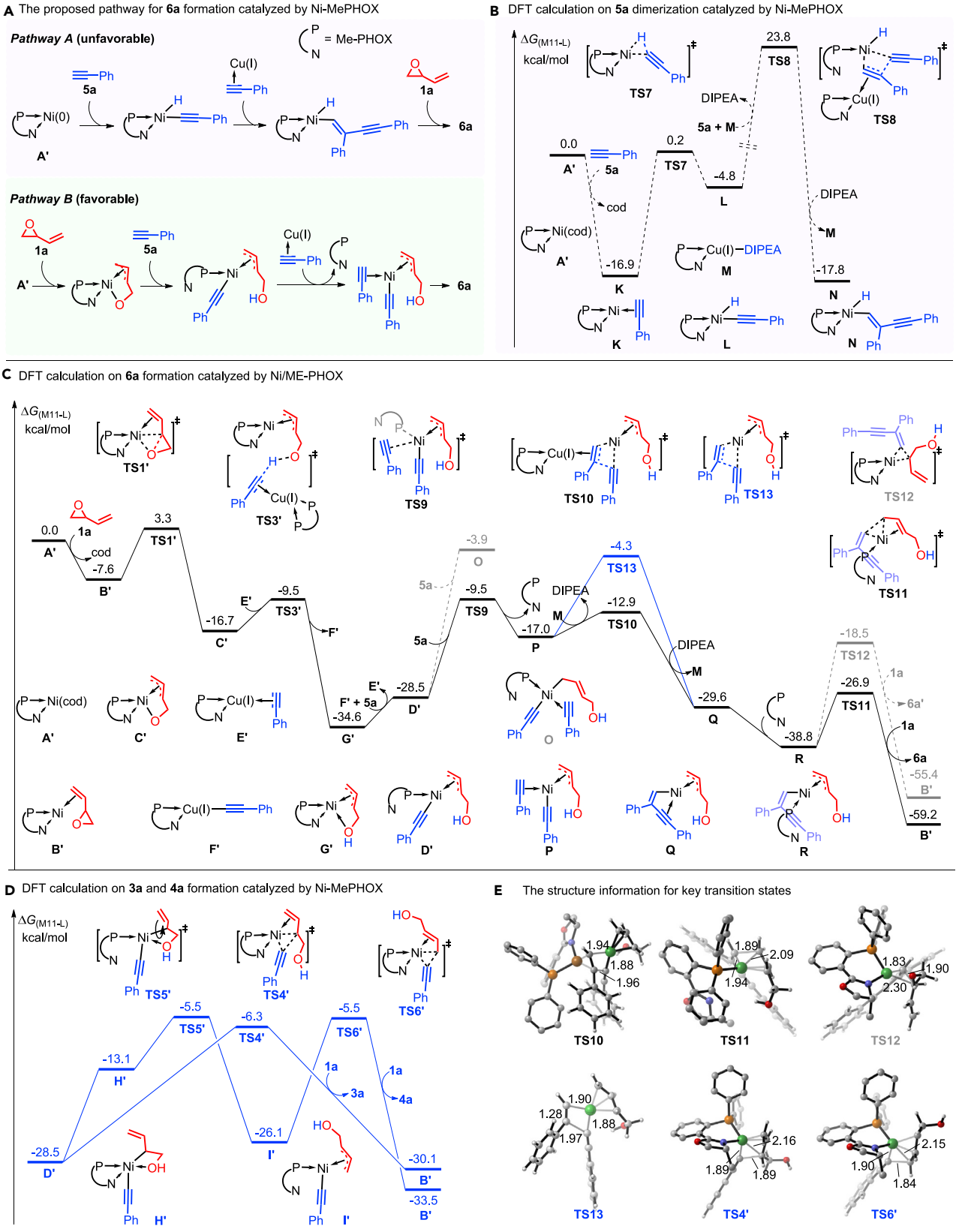
A The proposed pathway for 6a formation catalyzed by Ni-MePHOX
Pathway A (unfavorable)
P = Me-PHOX
Cu(I)
5a
1a
6a
A'
Pathway B (favorable)
B DFT calculation on 5a dimerization catalyzed by Ni-MePHOX
ΔG(M11-L) kcal/mol
TS7
TS8
DIPEA
5a + M
0.0
0.2
-4.8
L
-16.9
K
-17.8
N
M
cod
Ni(cod)
Cu(I)–DIPEA
C DFT calculation on 6a formation catalyzed by Ni/ME-PHOX
TS1'
TS3'
TS9
TS10
TS13
TS12
TS11
3.3
-7.6
B'
-16.7
C'
E'
-9.5
TS3'
F'
-34.6
G'
F' + 5a
-28.5
D'
-3.9
O
-17.0
P
-4.3
-12.9
-29.6
Q
-38.8
R
-18.5
-26.9
-55.4
-59.2
6a'
D DFT calculation on 3a and 4a formation catalyzed by Ni-MePHOX
TS5'
TS4'
TS6'
-5.5
-6.3
-13.1
H'
-26.1
I'
-30.1
-33.5
3a
4a
E The structure information for key transition states
1.94
1.88
1.96
1.89
2.09
1.94
1.83
1.90
2.30
1.90
1.28
1.97
1.88
2.16
1.89
1.89
2.15
1.90
1.84

Figure 4. Proposed pathway for 6a formation and DFT calculations on 5a dimerization, 6a, or 3a/4a formation catalyzed by Ni/Cu-Me-PHOX

(A) The proposed pathways for **6a** formation catalyzed by Ni/Me-PHOX. The typical stepwise alkyne dimerization followed by allylic alkylation (pathway **A**) was determined to be unfavorable by DFT calculations. The alternative trimolecular reaction (pathway **B**) was identified to be the favorable reaction pathway.

(B) The dimerization of **5a** catalyzed by Ni/Me-PHOX was energetically unfavorable as determined by DFT calculations.

(C) The Gibbs energy profiles for **6a** formation through a trimolecular Ni-catalyzed pathway assisted by Cu co-catalyst. Ligand dissociation from **D′** takes place to allow the formation of key intermediate **P** with the coordination of three molecules of substrates.

(D) The Gibbs energy profiles for **3a** and **4a** formation catalyzed by Ni/Me-PHOX as a comparison.

(E) Structure information of the key intermediates for the reaction profiles.

of the mechanistic studies (Figure 2D), alkyne dimerization should precede allylic alkylation. A stepwise pathway **A** (Figure 4A) was considered first, which includes oxidative addition of alkyne **5a** onto Ni(0) **A′**, migratory insertion to another **5a** followed by allylic alkylation of **1a**. To probe the feasibility of this mechanism, the Gibbs energy profiles for **5a** dimerization using nickel/copper cooperative catalysis was calculated first (Figure 4B). Ligand exchange of phenylacetylene **5a** with cyclooctadiene in **A′** gave π-complex **K** with exergonic of 16.9 kcal/mol. Subsequent oxidative addition of a C–H bond in **5a** onto Ni(0) center occurred via transition state **TS7** with a free energy barrier of 17.1 kcal/mol to generate the alkynyl-Ni(II) intermediate **L**. The following migratory insertion of phenylacetylene into C(alkynyl)-Ni(II) bond, activated by Cu(I) as a π-acid, took place via transition state **TS8** to generate the dimer alkenyl-Ni(II) intermediate **N**. The overall free energy barrier for **5a** dimerization is 40.7 kcal/mol. Such an inhibitively high barrier indicates that this pathway is unlikely the operating mechanism for the formation of **6a**. As the high activation barrier for **5a** dimerization partly comes from an unfavorable oxidative addition of terminal alkyne onto Ni(0) (**TS7** in Figure 4B), we hypothesized an alternative mechanism as shown in pathway **B** in Figure 4A. The key factor was the involvement of vinyl epoxide at the beginning to convert Ni(0) to Ni-π-allyl alkoxide complex, which then engages alkyne **5a** via alkoxide-assisted ligand exchange, analogous to that in Figure 3. Another alkyne coordination to the Ni-acetylide then set the stage for migratory insertion followed by allylic alkylation to form **6a**. DFT calculations were then carried out to probe the feasibility of this mechanism.

As shown in Figure 4C, coordination of vinyl epoxide **1a** to **A′** to give **B′**, oxidative addition to give **C′**, deprotonation of **E′** with **C′** followed by transmetalation produced alkynyl-Ni(II) complex **D′** with a similar potential energy surface to that in Figure 3 (via **TS3′**). It is noteworthy that the nitrogen atom in Me-PHOX does not coordinate with the Ni(II) center in **D′**. At this stage, coordination of another alkyne directly could form intermediate **O** with 24.6 kcal/mol endergonic. In contrast, an alternative alkyne coordination with the release of Me-PHOX ligand was identified to be energetically favorable, leading to **P** via **TS9** with an energy barrier of 19.0 kcal/mol. The hemilabile property of this P,N-ligand was a key factor for this intriguing new pathway to take place.

From intermediate **P**, migratory insertion of the acetylide ligand onto the alkyne, activated by Cu(I) as a π-acid, occurred via transition state **TS10** to give the alkenyl-Ni(II) intermediate **Q** with a free energy barrier of 4.1 kcal/mol. In **TS10**, the lengths of the forming C-C bond and C-Ni(II) bond are 1.96 and 1.94Å, respectively. Re-association of the Me-PHOX ligand with nickel center in **Q** to replace the alkyne coordination generated intermediate **R** with 9.2 kcal/mol exergonic. The following C(alkenyl)-C(allyl terminal) reductive elimination occurred via transition state **TS11** with a barrier of 11.9 kcal/mol to give terminal alkenylation **6a**. In transition state **TS11**, the length of the forming C(alkenyl)-C(allyl) bond is 1.89 Å. For the formation of internal alkenylation product **6a′**, reductive elimination had to take place via

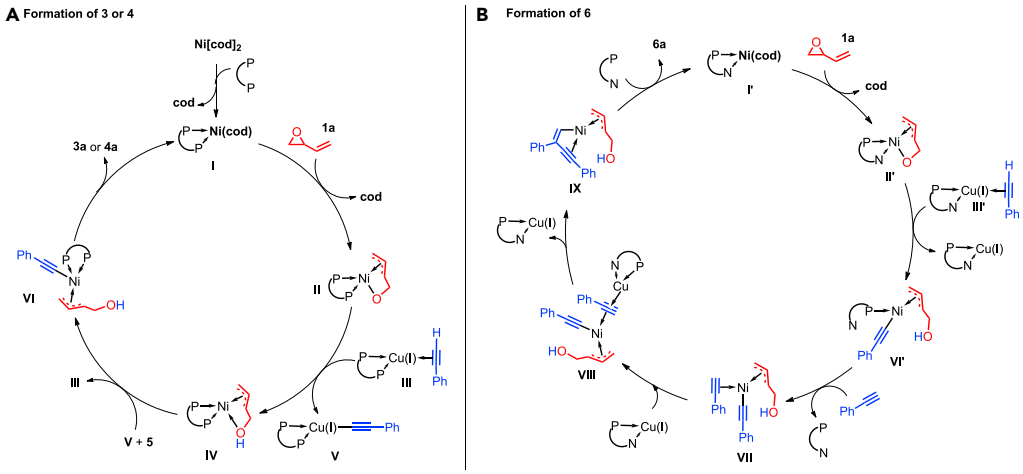

Figure 5. Proposed divergent catalytic pathways for the formation of 3/4 or 6 using bisphosphine or P,N-ligand

transition state **TS12** bearing a η-1 allyl unit with a free energy barrier of 20.3 kcal/mol. The much higher free energy of **TS12** versus **TS11** (8.4 kcal/mol) was consistent with experimental observation of the exclusive formation of linear **6a** (without the corresponding branched regioisomer). Overall, this pathway proceeded through an intriguing mechanism involving the dynamic association and dissociation of the hemilabile P,N-ligand, enabling an efficient trimolecular reaction.

To provide further support for the exclusive formation of **6a** (but not **3a**/**4a**) under our catalytic conditions, the formation of **3a** and **4a** catalyzed by Ni-MePHOX was also calculated. As illustrated in Figure 4D, a similar pathway to that in Figure 3 was determined to be the case. Notably, the weak coordination capacity of the nitrogen atom in Me-PHOX resulted in a similar free energy of **TS4′** and **TS5′** that would lead to the formation of **3a** and **4a** as a mixture. However, the activation barrier of **TS10** for **6a** formation (Figure 4C) was much lower than that of **TS4′** and **TS5′**, which is experimentally consistent with the exclusive formation of **6a**.

As shown by the control experiment in Figure 2C, right, the presence of copper co-catalyst made a significant difference for the product distribution of this reaction using Ni-MePHOX catalyst. Instead of exclusive **6a** formation in the presence of copper, **3a**, **4a**, and **6a** were formed in equal amounts in the absence of CuI. To better understand the effect of CuI, the activation barrier for the migratory insertion step in **6a** formation was further calculated without activation by copper. As shown by **TS13** in Figure 4C, the activation barrier (24.2 kcal/mol from **D′**) was determined to be comparable to that of **TS4′** and **TS5′** (22.2/23.0 kcal/mol from **D′**). Thus, this agrees well with the mechanistic studies with or without copper co-catalyst.

To provide a full picture of this ligand-induced divergent reaction system, the ligand-dissociation pathway for trimolecular reaction with XantPhos, experimentally not observed, was also probed by DFT calculation (see Figure S132). The activation barrier for the ligand-dissociation pathway analogous to that in Figure 4C with bisphosphine was determined to be much less favorable. Overall, these data from DFT calculations provided a conclusive overall picture for this ligand-induced divergent allylic alkylation.

Based on the above DFT calculations, the catalytic pathways for the ligand-induced divergent synthesis of **3/4** or **6** are summarized in Figures 5A and 5B for direct

comparison. Most notably, the dynamic dissociation of hemilabile P,N-ligand from VI′ enabled the formation of the key intermediate VII (Figure 5B), from which a trimolecular reaction takes place, leading to the formation of product **6**.

Scope of divergent allylic alkylation of vinyl epoxides and aziridines with alkynes

With the optimal conditions in hand, we turned our attention to exploring the scope of these ligand-induced divergent allylic alkylations. As illustrated in Figure 6, it is important to note that the only variation in the reaction parameters leading to different product formation was the identity of the ligand.

Allylic alkynylation of vinyl epoxides to yield skipped enynes was explored first. The scope of terminal alkynes for this transformation turned out to be remarkably broad (Figure 6A). Under the same set of optimal conditions, a wide range of phenylacetylene derivatives **5** bearing substituents of different electronic characters on different positions of the aryl ring underwent efficient alkynylation to produce **3a–3g** in good to high yields. Terminal alkynes bearing heterocyclic substituents, such as pyridine, imidazole, and thiophene, all participated in the alkynylation reaction smoothly to yield **3h–3j** in high yields. Furthermore, alkenyl-, alkyl-, and silyl-substituted alkynes were good substrates as well (70%–83% for **3k–3m**). More importantly, a wide spectra of common functionalities such as chloro-, cyano-, acetyl-, and hydroxyl-amines were all well tolerated to deliver **3n–3u** in 65%–85% yields. The generality of this method prompted us to examine alkyne-containing complex drug compounds for the alkynylation as well. As a representative example, the tyrosine kinase inhibitor erlotinib[28] underwent a smooth reaction to yield **3v** in 66% yield. With a simple procedure utilizing commercially available catalysts and reagents, we are confident that this method may find wide use as a reliable modification of terminal alkynes bearing diverse substituents.

To our delight, this catalytic system was also successfully extended to the alkynylation of vinyl aziridine **7** (Figure 6B). Under the same set of optimal conditions, various terminal alkynes participated in the reaction smoothly. As shown by the representative examples, aryl-, heteroaryl-, and alkyl-substituted terminal alkynes were all suitable nucleophiles to produce the amine-containing 1,4-enynes **8** in good efficiency and excellent regioselectivity.

The scope of the synthesis of dienynes **6** was explored next (Figure 6C). It is noteworthy that a single geometric isomer at the tri-substituted alkene was observed for all cases. A wide range of aryl- and heteroaryl-alkynes participated in this reaction to produce **6a–6k** in good to excellent yields. Alkenyl-substituted alkynes also could be used to yield **6l** and **6m** in good yields. As one limitation for this series, alkyl-substituted alkynes failed to undergo reactions to produce the desired products **6**. Moreover, we were delighted to find that this transformation could also tolerate substituted vinyl epoxides. Compounds **6n** and **6o** could be produced from **1b** and **1c** in good to high yields. The conversion of vinyl aziridine **7** to allyl amine **9** also proceeded smoothly under the standard conditions. The general scope, coupled with a simple procedure, makes this reaction a useful method for the preparation of these synthetically valuable functionalized enyne-containing allyl alcohols and amines.

Allylic alkynylation of vinyl ethylene carbonates to yield products bearing a quaternary center

To further expand the scope of this methodology, we aimed toward the synthesis of skipped enynes bearing a quaternary center (**10** in Figure 7). However, these efforts were met with much trouble by the use of substituted vinyl epoxide, such as **1d**,

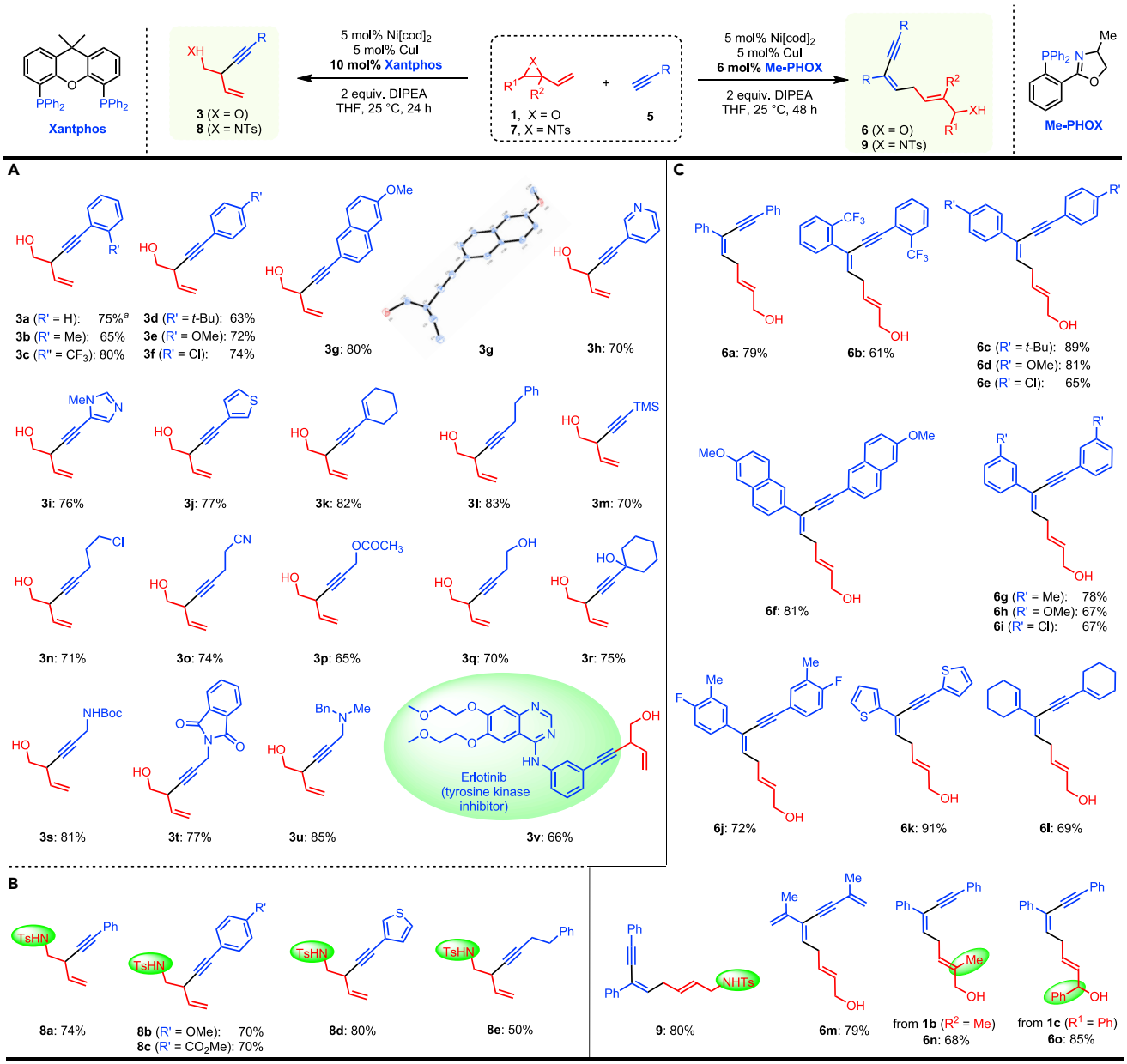

Figure 6. The scope of divergent allylic alkylation of vinyl epoxides/aziridines with alkynes

The reactions were carried out on a 0.2 mmol scale. Isolated yields of the pure products were reported. See Supplemental information for the detailed reaction conditions.

(A) In the presence of Xantphos ligand, highly efficient and regioselective allylic alkynylation of vinyl epoxides is achieved with a wide range of alkynes bearing various functionalities. The reactions were carried out using 2 equiv of alkynes versus vinyl epoxides. [a]For this reaction, NiXantphos was used as the ligand due to the separation issue of Xantphos from the desired product. The use of TBME as the solvent was beneficial over THF to yield **3a** in 75% isolated yield.

(B) Allylic alkynylation of vinyl aziridines worked with the same efficiency and selectivity to deliver skipped enynes bearing an amine functionality.

(C) In the presence of Me-PHOX ligand, a wide range of alkynes and vinyl epoxides and aziridines underwent smooth reaction to deliver the trimolecular products **6** and **9** in high efficiency. The reactions were carried out using 3 equiv of alkynes versus vinyl epoxides.

which underwent epoxide to aldehyde rearrangement under the standard conditions instead of alkynylation to deliver the desired 1,4-enyne **10a** (Figure 7A). In an effort to overcome this problem, we turned our attention to the related vinyl ethylene carbonate (VEC) **11**, which is known to be less prone to rearrangement

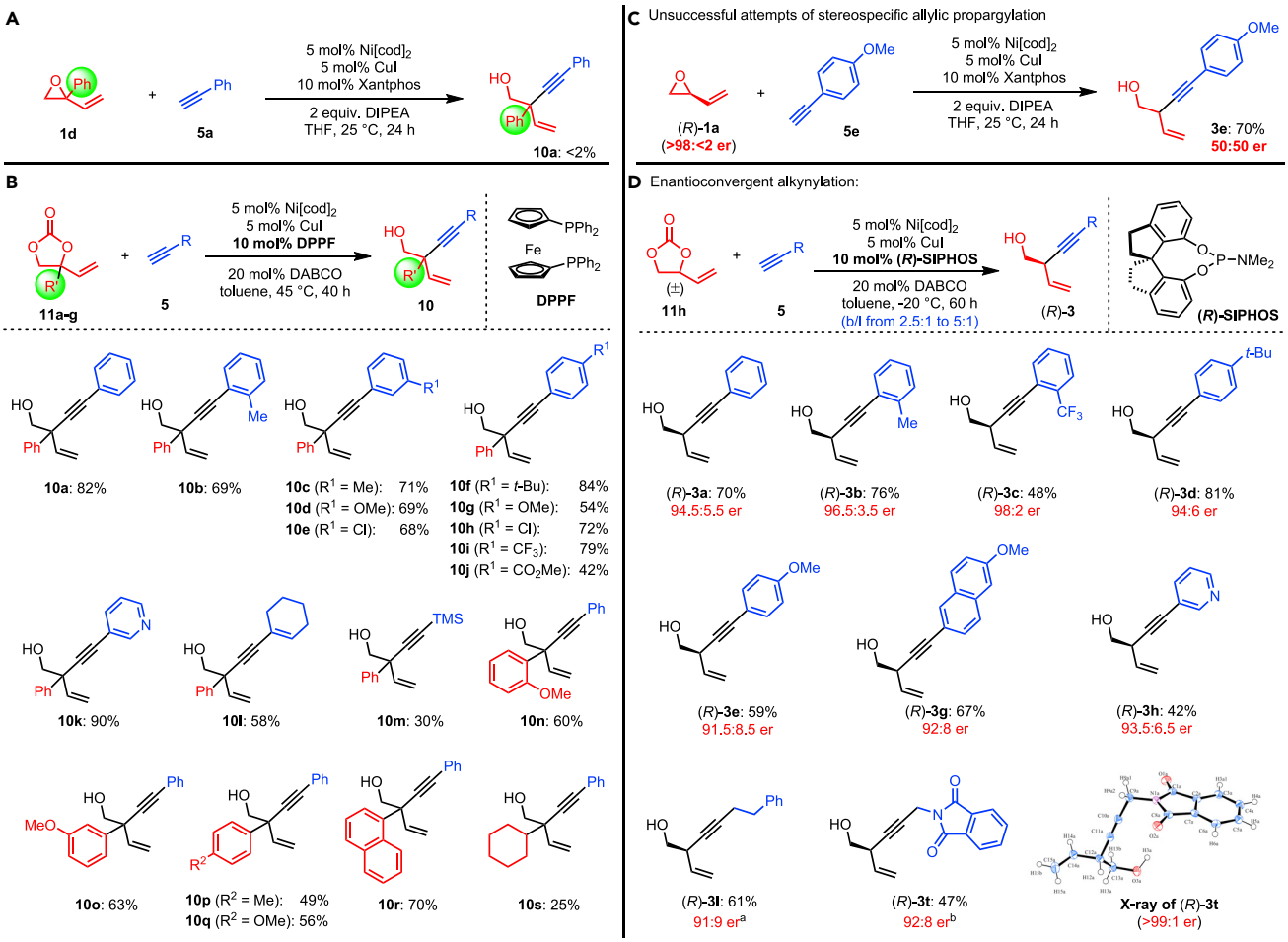

Figure 7. Reactions of vinyl ethylene carbonates (VECs) to access products bearing a quaternary center and enantioselective allylic alkynylation

(A) The allylic alkynylation of substituted vinyl epoxide **1d** failed due to alternative side reaction.

(B) By the use of aryl-substituted VECs as the substrate, the allylic alkynation proceeded smoothly to yield 10 bearing a quaternary center in good to high efficiency. Further optimization identified DPPF and DABCO as the best choices of ligand and base. See Supplemental information for detailed reaction conditions.

(C) The allylic alkynylation of enantiopure **1a** led to the formation of racemic product **3e**, suggesting a stereoablative pathway via Ni-π-allyl intermediate.

(D) An enantioconvergent allylic alkynylation of VECs **11** produced enantioenriched skipped enynes **3** in good to excellent yields and enantioselectivities. (*R*)-SIPHOS was identified to be the optimal chiral ligand for this transformation. A lower temperature of −20°C was needed to achieve high enantioselectivity. Under these conditions, the branched to linear ratio ranged from 2.5:1 to 5:1, and the pure branched product **3** was isolated in pure form. See Supplemental information for detailed reaction conditions. [a]The reaction used 10 mol % nickel and copper and 20 mol % ligand and the reaction time was 120 h. [b]Ambient temperature was used for this reaction due to the low solubility of this terminal alkyne substrate.

under Lewis acidic conditions and may provide a different chemo-selectivity to favor the desired allylic alkynylation. It is noteworthy that allylic substitution of these compounds using heteroatom-based nucleophiles including enantioselective variants has been well-established in recent years.[29–34] In contrast, the use of carbon-nucleophiles in this reaction remains rare in the literature.[35]

The allylic alkynylation of **11a** (R′ = Ph) using **5a** under the standard conditions from Figure 6A turned out to be very sluggish, leading to minimal formation of the desired **10a**. After much optimization (see Supplemental information for details), the use of DPPF as the ligand and a stronger base—DABCO—proved to be important for an

efficient Ni/Cu-catalyzed alkynylation of **11** to deliver **10** in high efficiency. As shown in Figure 7B, **10a** was produced in a good yield of 82%. Similar to the previous substrate scope, alkynes bearing different aryl, heteroaryl, alkenyl, and silyl substituents were all well tolerated in this reaction to yield **10b–10m** in good to high yields. In addition, various aryl-substituted VECs underwent reactions smoothly to deliver **10n–10r** in moderate to good yields. VEC with a cyclohexyl group could also participate in this reaction, albeit with a low yield for **10s**.

Enantioconvergent allylic alkynylation of vinyl ethylene carbonates

In nickel-catalyzed allylic alkylation or cross coupling of aryl ethers, both pathways of stereospecific transfer of the substrate chirality to the product[36] and stereoablative synthesis of enantioenriched products have been reported.[37] When we tested allylic alkynylation using the enantiopure vinyl epoxide **1a** under the standard conditions (Figure 7C), product **3e** was obtained in a racemic form in 70% yield. This suggests that the nickel-π-allyl intermediate for this catalytic alkynylation is prone to racemization. This observation prompted us to explore an enantioconvergent synthesis of the valuable skipped enynes. Again, much optimization with vinyl epoxide **1a** led to low conversion to the desired product **3a** by the use of various chiral ligands. Further extensive optimization with VEC **11h** (see Supplemental information for details) identified that the use of (*R*)-SIPHOS and DABCO at −20°C produced **3a** in good yield and high enantioselectivity (70% yield, 94.5:5.5 er; Figure 7D). The scope of this enantioselective allylic alkynylation was then explored. A broad scope of terminal alkynes was achieved. Arylalkynes bearing different substituents underwent efficient alkynylation to yield **3a–3g** with up to 98:2 er. Pyridyl-containing alkyne worked similarly well to produce **3h** in 93.5:6.5 er, albeit with a slightly reduced yield. Alkynes bearing alkyl substituents turned out to be much less reactive. A higher catalyst loading plus longer reaction time or higher temperature was necessary to produce **3l** and **3t** in reasonable yield and good 91:9 or 92:8 er. The enantioselective alkynylation of substituted VEC **11a** was also attempted. However, no reactivity was obtained for these bulkier substrates. It is noteworthy that in these enantioselective reactions, the branched to linear regioselectivity was lower than the racemic series in Figure 6A. However, the pure branched products could be easily obtained by chromatography separation. The absolute configuration of **3t** was assigned unambiguously by single crystal X-ray analysis.

Conclusions

We present herein an unprecedented Ni/Cu-catalyzed allylic alkynylation of vinyl epoxides, vinyl carbonates, and vinyl aziridines using readily available terminal alkynes. The scope of this catalytic method, especially toward the alkynes, is remarkably broad. The enantioselective variant of this process has also been realized. By switching to a hemilabile P,N-ligand, the formation of enyne-containing allyl alcohols and amines from a trimolecular reaction was also realized with a broad scope. For this intriguing ligand effect leading to divergent bimolecular or trimolecular reactivities, evidence from DFT calculations pointed to the dynamic ligand coordination/dissociation, which influenced the number of open sites on the metal center at an appropriate stage in the catalysis to bind varied number of substrates and induce different reactivities. With this important discovery, further application of this valuable principle for divergent transition metal catalysis will be explored in our laboratories.

EXPERIMENTAL PROCEDURES

Resource availability

Lead contact

Further information and requests for resources should be directed to and will be fulfilled by the lead contact, Yu Zhao (zhaoyu@nus.edu.sg).

Materials availability

All unique reagents generated in this study are available from the Lead Contact without restriction.

Data and code availability

All data needed to support the conclusions of this manuscript are included in the main text or Supplemental information. Crystallographic data generated during this study have been deposited in the Cambridge Crystallographic Data Centre (CCDC) under accession numbers CCDC:1920222 (3g) and 1920233 (R-3t). These data can be obtained free of charge from the CCDC at http://www.ccdc.cam.ac.uk/data_request/cif.

Representative procedure Ni/Cu-catalyzed alkynylation of vinyl epoxides

To a vial equipped with a dried stir bar was added Ni[cod]$_2$ (0.01 mmol), Xantphos (0.02 mmol), and anhydrous THF (1.0 mL) in the glovebox. The reaction mixture was then allowed to stir for 15 min, followed by the addition of CuI (0.01 mmol), vinyl epoxide **1a** (0.20mmol), acetylene **5a** (0.40 mmol), and DIPEA (0.40 mmol). The reaction tube was sealed and taken outside the glovebox and allowed to stir at room temperature for 24 h. The crude reaction mixture was concentrated under reduced pressure and directly purified by silica gel chromatography (ethyl acetate/hexanes = 1:8).

SUPPLEMENTAL INFORMATION

Supplemental information can be found online at https://doi.org/10.1016/j.chempr.2021.02.018.

ACKNOWLEDGMENTS

We are grateful for the financial support from Ministry of Education of Singapore (R-143-000-A94-112), National University of Singapore (R-143-000-A57-114), Xi'an Jiaotong University Youth Talent Support Program (0800-712110510716), National Natural Science Foundation of China (21901066, 21822303, and 22001203), and the 111 Project (D20003). We acknowledge the allocation of computing resources at the Henan Province Supercomputing Center.

AUTHOR CONTRIBUTIONS

Y.H. and C.M. designed and performed the experimental work, with help from L.-C.Y.; S.L. and Y.L. performed the DFT calculation. Y.Z. directed the project and wrote the manuscript with Y.H., C.M., S.L., and Y.L.

DECLARATION OF INTERESTS

The authors declare no competing interests.

Received: September 15, 2020
Revised: December 13, 2020
Accepted: February 12, 2021
Published: March 11, 2021

REFERENCES

1. O'Connor, C.J., Beckmann, H.S.G., and Spring, D.R. (2012). Diversity-oriented synthesis: producing chemical tools for dissecting biology. Chem. Soc. Rev. *41*, 4444–4456.

2. Mahatthananchai, J., Dumas, A.M., and Bode, J.W. (2012). Catalytic selective synthesis. Angew. Chem. Int. Ed. Engl. *51*, 10954–10990.

3. Krautwald, S., and Carreira, E.M. (2017). Stereodivergence in asymmetric catalysis. J. Am. Chem. Soc. *139*, 5627–5639.

4. Beletskaya, I.P., Nájera, C., and Yus, M. (2018). Stereodivergent catalysis. Chem. Rev. *118*, 5080–5200.

5. Nájera, C., Beletskaya, I.P., and Yus, M. (2019). Metal-catalyzed regiodivergent organic reactions. Chem. Soc. Rev. *48*, 4515–4618.

6. Trost, B.M., and Crawley, M.L. (2003). Asymmetric transition-metal-catalyzed allylic alkylations: applications in total synthesis. Chem. Rev. *103*, 2921–2944.

7. Lu, Z., and Ma, S. (2008). Metal-catalyzed enantioselective allylation in asymmetric synthesis. Angew. Chem. Int. Ed. Engl. *47*, 258–297.

8. Butt, N.A., and Zhang, W. (2015). Transition metal-catalyzed allylic substitution reactions with unactivated allylic substrates. Chem. Soc. Rev. *44*, 7929–7967.

9. Hethcox, J.C., Shockley, S.E., and Stoltz, B.M. (2016). Iridium-catalyzed Diastereo-, enantio-, and regioselective allylic alkylation with prochiral enolates. ACS Catal *6*, 6207–6213.

10. Cheng, Q., Tu, H.F., Zheng, C., Qu, J.P., Helmchen, G., and You, S.L. (2019). Iridium-catalyzed asymmetric allylic substitution reactions. Chem. Rev. *119*, 1855–1969.

11. Dutta, S., Bhattacharya, T., Werz, D.B., and Maiti, D. (2020). Transition metal catalyzed C-H allylation reactions. Chem. https://doi.org/10.1016/j.chempr.2020.10.020.

12. Dabrowski, J.A., Gao, F., and Hoveyda, A.H. (2011). Enantioselective synthesis of alkyne-substituted quaternary carbon stereogenic centers through NHC-Cu-catalyzed allylic substitution reactions with $(i\text{-Bu})_2$(alkynyl) aluminum reagents. J. Am. Chem. Soc. *133*, 4778–4781.

13. Hamilton, J.Y., Sarlah, D., and Carreira, E.M. (2013). Iridium-catalyzed enantioselective allylic alkynylation. Angew. Chem. Int. Ed. Engl. *52*, 7532–7535.

14. Harada, A., Makida, Y., Sato, T., Ohmiya, H., and Sawamura, M. (2014). Copper-catalyzed enantioselective allylic alkylation of terminal alkyne pronucleophiles. J. Am. Chem. Soc. *136*, 13932–13939.

15. Cui, X.Y., Ge, Y., Tan, S.M., Jiang, H., Tan, D., Lu, Y., Lee, R., and Tan, C.H. (2018). (Guanidine) copper complex-catalyzed enantioselective dynamic kinetic allylic alkynylation under biphasic condition. J. Am. Chem. Soc. *140*, 8448–8455.

16. Huang, W.Y., Lu, C.H., Ghorai, S., Li, B., and Li, C. (2020). Regio- and enantioselective allylic alkylation of terminal alkynes by synergistic Rh/Cu catalysis. J. Am. Chem. Soc. *142*, 15276–15281.

17. Li, Y.X., Xuan, Q.Q., Liu, L., Wang, D., Chen, Y.J., and Li, C.J. (2013). A Pd(0)-catalyzed direct dehydrative coupling of terminal alkynes with allylic alcohols to access 1,4-enynes. J. Am. Chem. Soc. *135*, 12536–12539.

18. He, J., Ling, J., and Chiu, P. (2014). Vinyl epoxides in organic synthesis. Chem. Rev. *114*, 8037–8128.

19. Guo, W., Gómez, J.E., Cristòfol, À., Xie, J., and Kleij, A.W. (2018). Catalytic transformations of functionalized cyclic organic carbonates. Angew. Chem. Int. Ed. Engl. *57*, 13735–13747.

20. Ohno, H. (2014). Synthesis and applications of vinylaziridines and ethynylaziridines. Chem. Rev. *114*, 7784–7814.

21. Tasker, S.Z., Standley, E.A., and Jamison, T.F. (2014). Recent advances in homogeneous nickel catalysis. Nature *509*, 299–309.

22. Pye, D.R., and Mankad, N.P. (2017). Bimetallic catalysis for C-C and C-X coupling reactions. Chem. Sci. *8*, 1705–1718.

23. Wu, Y., Huo, X., and Zhang, W. (2020). Synergistic Pd/Cu catalysis in organic synthesis. Chemistry *26*, 4895–4916.

24. Trost, B.M., Bunt, R.C., Lemoine, R.C., and Calkins, T.L. (2000). Dynamic kinetic asymmetric transformation of diene monoepoxides: a practical asymmetric synthesis of Vinylglycinol, vigabatrin, and ethambutol. J. Am. Chem. Soc. *122*, 5968–5976.

25. Du, C., Li, L., Li, Y., and Xie, Z. (2009). Construction of two vicinal quaternary carbons by asymmetric allylic alkylation: total synthesis of hyperolactone C and (−)-biyouyanagin A. Angew. Chem. Int. Ed. Engl. *48*, 7853–7856.

26. Ma, C., Huang, Y., and Zhao, Y. (2016). Stereoselective 1,6-conjugate addition/annulation of para-quinone methides with vinyl epoxides/cyclopropanes. ACS Catal *6*, 6408–6412.

27. Frisch, M.J., Trucks, G.W., Schlegel, H.B., Scuseria, G.E., Robb, M.A., Cheeseman, J.R., Scalmani, G., Barone, V., Petersson, G.A., Nakatsuji, H., et al. (2013). Gaussian 09, revision D.01, Gaussian. The full author list is shown in Supporting information.

28. Dowell, J., Minna, J.D., and Kirkpatrick, P. (2005). Erlotinib hydrochloride. Nat. Rev. Drug Discov. *4*, 13–14.

29. Guo, W., Martínez-Rodríguez, L., Kuniyil, R., Martin, E., Escudero-Adán, E.C., Maseras, F., and Kleij, A.W. (2016). Stereoselective and versatile preparation of tri- and tetrasubstituted allylic amine scaffolds under mild conditions. J. Am. Chem. Soc. *138*, 11970–11978.

30. Cai, A., Guo, W., Martínez-Rodríguez, L., and Kleij, A.W. (2016). Palladium-catalyzed Regio- and enantioselective synthesis of allylic amines featuring tetrasubstituted tertiary carbons. J. Am. Chem. Soc. *138*, 14194–14197.

31. Khan, A., Khan, S., Khan, I., Zhao, C., Mao, Y., Chen, Y., and Zhang, Y.J. (2017). Enantioselective construction of tertiary C-O bond via allylic substitution of Vinylethylene carbonates with water and alcohols. J. Am. Chem. Soc. *139*, 10733–10741.

32. Khan, A., Zhao, H., Zhang, M., Khan, S., and Zhao, D. (2020). Regio- and enantioselective synthesis of sulfone-bearing quaternary carbon stereocenters by Pd-catalyzed allylic substitution. Angew. Chem. Int. Ed. Engl. *59*, 1340–1345.

33. Rong, Z.Q., Yang, L.C., Liu, S., Yu, Z., Wang, Y.N., Tan, Z.Y., Huang, R.Z., Lan, Y., and Zhao, Y. (2017). Nine-membered benzofuran-fused heterocycles: enantioselective synthesis by Pd-catalysis and rearrangement via transannular bond formation. J. Am. Chem. Soc. *139*, 15304–15307.

34. Wang, Y.N., Yang, L.C., Rong, Z.Q., Liu, T.L., Liu, R., and Zhao, Y. (2018). Pd-catalyzed enantioselective [6+4] cycloaddition of vinyl oxetanes with azadienes to access ten-membered heterocycles. Angew. Chem. Int. Ed. Engl. *57*, 1596–1600.

35. Khan, A., Yang, L., Xu, J., Jin, L.Y., and Zhang, Y.J. (2014). Palladium-catalyzed asymmetric decarboxylative cycloaddition of vinylethylene carbonates with Michael acceptors: construction of vicinal quaternary stereocenters. Angew. Chem. Int. Ed. Engl. *53*, 11257–11260.

36. Zhou, Q., Srinivas, H.D., Zhang, S., and Watson, M.P. (2016). Accessing both retention and inversion pathways in stereospecific, nickel-catalyzed Miyaura borylations of allylic pivalates. J. Am. Chem. Soc. *138*, 11989–11995.

37. Son, S., and Fu, G.C. (2008). Nickel-catalyzed asymmetric Negishi cross-couplings of secondary allylic chlorides with alkylzincs. J. Am. Chem. Soc. *130*, 2756–2757.